Effect of mid-term drought on *Quercus pubescens* BVOCs emissions seasonality and their dependence to light and/or temperature

Amélie Saunier[1], Elena Ormeño[1], Christophe Boissard[2], Henri Wortham[3], Brice Temime-Roussel[3], Caroline Lecareux[1], Alexandre Armengaud[4], Catherine Fernandez[1].

[1]Aix Marseille Univ, Univ Avignon, CNRS, IRD, IMBE, Marseille, France.

[2]Laboratoire des Sciences du Climat et de l'Environnement, LSCE/IPSL, CEA-CNRS-UVSQ, Université Paris-Saclay, F-91191 Gif-sur-Yvette, France.

[3]Aix Marseille Univ, CNRS, LCE, Laboratoire de Chimie de l'Environnement, Marseille, France

[4] Air PACA, 146 rue Paradis, Bâtiment Le Noilly Paradis, 13294 Marseille, Cedex 06.

Correspondence to: Amélie Saunier (amelie.saunier@imbe.fr)

Key words: BVOCS, natural and amplified drought, season, light and temperature

Abstract. Biogenic volatile organic compounds (BVOCs) emitted by plants represent a large source of carbon compounds released into the atmosphere where they account for precursors of tropospheric ozone and secondary organic aerosols. Being directly involved in air pollution and indirectly in climate change, understanding what factors drive BVOC emissions is a prerequisite for modelling their emissions and predict air pollution. The main algorithms currently used to model BVOCs emissions are mainly light and/or temperature dependent. Additional factors such as seasonality and drought also influence isoprene emissions, especially in the Mediterranean region which is characterized by a rather long drought period in summer. These factors are increasingly included in models but only for the principal studied BVOC, namely isoprene but there are still some discrepancies in estimations of emissions. In this study, the main BVOCs emitted by *Quercus pubescens*: isoprene, methanol, acetone, acetaldehyde, formaldehyde, MACR, MVK and ISOPOOH (these 3 last compounds detected under the same ion), were monitored with a PTR-ToF-MS over an entire seasonal cycle, under both *in situ* natural and amplified drought which is expected with climate change. Amplified drought impacted all studied BVOCs by reducing emissions in spring and summer while increasing emissions in autumn. All six BVOCs monitored showed daytime light and temperature dependencies while three BVOCs (methanol, acetone and formaldehyde) also showed emissions during the night despite the absence of light under constant temperature. Moreover, methanol and acetaldehyde burst in the early morning and formaldehyde deposition/uptake were also punctually observed which were not assessed by the classical temperature and light models.

1 Introduction

Plants contribute to global emissions of volatile organic compounds (VOCs) with an estimated emission rate of 10^{15} gC yr^{-1} (Guenther *et al.* 1995; Harrison *et al.* 2013). The large variety of compounds released by plants represents, at the global scale, 2-3% of the total carbon released in the atmosphere (Kesselmeier & Staudt 1999). Under strong photochemical conditions, BVOCs, together with NO_x, can significantly contribute to tropospheric ozone concentration (Xie *et al.* 2008; Papiez *et al.* 2009). In addition to its greenhouse effect, O_3 has strong effects on plant metabolism (Reig-Armiñana *et al.* 2004; Beauchamp *et al.* 2005) as well as on human health (Lippmann 1989). BVOCs are also rapidly oxidized by OH radical and NO_3 (Hallquist *et al.* 2009; Liu *et al.* 2012), which account for an important fraction of the total mass of secondary organic aerosols (SOA, Jimenez *et al.* 2009). Methanol and acetone are, after isoprene, the principal BVOC released to the atmosphere. Isoprene emissions represent between 400-600 TgC yr^{-1} at the global scale (Arneth *et al.* 2008) whereas methanol emissions vary between 75 and 280 TgC yr^{-1} (Singh *et al.* 2000; Heikes *et al.* 2002, respectively) and acetone emissions represent only 33 TgC yr^{-1} (Jacob *et al.* 2002). Other compounds such as acetaldehyde, methacrolein (MACR), methyl vinyl ketone (MVK), isoprene hydroxy hydroperoxides (ISOPOOH) and formaldehyde, whose biogenic origin has been poorly investigated, are better known to be anthropogenic and/or secondary VOCs issued from atmospheric oxidations (Hallquist *et al.* 2009). However, acetaldehyde is also a by-product of plant metabolism and its emissions represent 23 Tg yr^{-1} at the global scale (Millet *et al.* 2010). Formaldehyde, MACR, MVK and ISOPOOH are released by plants through oxidations of methanol and isoprene, respectively, within leaves but they can have other leaf precursors (Oikawa & Lerdau 2013). Thus, it is thereby important to model all this panel of BVOCs emissions with the aim of predicting their effect on secondary atmospheric chemistry.

Current models allow to predict BVOCs emissions according to the type of vegetation, biomass density, leaf age, specific emission factor for many vegetal species, as well as the impact of some environmental factors. Models, such as the MEGAN (Guenther *et al.* 2006; Guenther *et al.* 2012) or CHIMERE (Menut *et al.* 2014) model, include at least two main algorithms that allow to model light and temperature emissions dependence (called *L+T* algorithm afterwards) and a temperature dependent algorithm (called *T* algorithm afterwards), both described in Guenther *et al.* (1995). The L+T algorithm is typically used for BVOCs emissions whose synthesis rapidly relies on photosynthesis, and hence include *de novo* emissions. The T algorithm is used for BVOCs emissions that do not directly rely on BVOCs synthesis when, for example, they originate from permanent large storage pools (Ormeno *et al.* 2011). The dependence to light and/or temperature is well documented for isoprenoids (Owen *et al.* 2002; Rinne *et al.* 2002; Dindorf *et al.* 2006) but there is still a lack of knowledge about highly volatile BVOCs (e.g. methanol, acetone, acetaldehyde). However, many of these compounds are very reactive in the atmosphere (Hallquist *et al.* 2009) and, could be emitted in large quantities to the atmosphere at global scale. The characterization of their emissions and sensitivity to light and/or temperature is, thus, necessary in order to obtain reliable predictions of atmospheric processes in order not to miss this important part of the atmospheric reactivity. Other factors than light and temperature can drive BVOCs emissions such as water stress. Most studies dealing with BVOCs response to water stress have, however, focused on terpene-like compounds and have been carried out after weeks of watering restriction or removal under controlled conditions (for a review, see studies cited in Peñuelas and Staudt 2010). Considerable uncertainty remains in our understanding of emission mechanisms since some works showed increases (Funk *et al.* 2004; Monson *et al.* 2007) or decreases of isoprene emissions (Brüggemann & Schnitzler 2002; Fortunati *et al.* 2008) and there is a lack of knowledge on the impact of water stress on highly BVOCs emissions. Moreover, the understanding of isoprene sensitivity and highly volatile BVOCs

71 to recurrent water stress (few years) under *in situ* conditions is clearly missing. Likewise, the capacity of current
72 *L+T* and *T* algorithms to predict emission shifts under different drought scenarios in the context of climate change
73 needs to be addressed for isoprene and highly volatile compounds. This is of especial interest for the Mediterranean
74 area where the most severe climatic scenario of the IPCC predicts an intensification of summer drought consisting
75 on a rain reduction that can locally reach 30%, an extension of the drought period as well as a temperature rise of
76 3.4°C, (Giorgi & Lionello 2008; IPCC 2013; Polade *et al.* 2014) for 2100.
77 In the present investigation, we aimed (i) to study the emission factors of each studied BVOC released by *Q.*
78 *pubescens,* including isoprene and highly volatile compounds that originate from plant metabolism under water
79 stress (ii) to test the performance of the L+T and T algorithms to predict isoprene and highly volatile BVOC
80 emissions over the seasonal cycle and under two recurrent water stress treatments. *Q. pubescens* was chosen as
81 vegetal model because this species is highly resistant to drought and well widespread in the Northern
82 Mediterranean area occupying 2 million ha (Quézel & Médail 2003). It also represents the major source of isoprene
83 emissions in the Mediterranean area and the second one at the European scale (Keenan *et al.* 2009).

84 **2 Material and methods**

85 **2.1 Experimental site**

86 Our study was performed at the O_3HP site (Oak Observatory at OHP, Observatoire de Haute Provence), located
87 60 km North of Marseille, France (5°42'44" E, 43°55'54" N), at an elevation of 650m above the sea level. The
88 O_3HP (955m^2), free from direct human disturbance for 70 years, is a homogeneous forest mainly composed of *Q.*
89 *pubescens* (≈ 90 % of the biomass and ≈ 75 % of the trees) with a mean diameter of 1.3 m. The remaining 10 %
90 of the biomass is mostly represented by *Acer monspessulanum* trees, a very low isoprene-emitter species (Genard-
91 Zielinski *et al.* 2015). The O_3HP site was created in 2009 in order to study the impact of climate change on a *Q.*
92 *pubescens* forest. Using a rainfall exclusion device (an automated monitored roof deployed during chosen rain
93 events) set up over part of the O_3HP canopy, it was possible to reduce natural rain by 30% and to extend the
94 drought period in an attempt to mimic the current climatic model projections for 2100 (Giorgi & Lionello 2008;
95 IPCC 2013; Polade et al. 2014). Two plots were considered in the site; a plot receiving natural precipitation where
96 trees grew under natural drought (300m² surface, used as control plot) and a second plot submitted to amplified
97 drought (232m² surface). Rain exclusion on this latter plot started on May 2012 and was continuously applied
98 every year, principally, during the growth period. Ombrothermic diagrams indicate that the drought period was
99 extended for 2 months in 2012, 4 months in 2013 and 3 months in 2014 for amplified drought relative to natural
100 drought (Fig 1). Data on cumulative precipitation show that 35% of rain was excluded in 2012 (from 29 April from
101 to 27 October), 33.5% in 2013 (from 7 July from to 29 December), 35.5% in 2014 (from 8 April to 8 December).
102 This experimental set up involved a recurrent drought in the amplified drought plot. Sampling was performed at
103 the branch-scale at the top of the canopy during three campaigns from October 2013 to July 2014, covering an
104 entire seasonal cycle: in autumn (14 to 28 October 2013, 2nd year of amplified drought), in spring (12 to 19 May
105 2014, 3rd year of amplified drought) and in summer (13 to 25 July 2014, 3rd year of amplified drought). Spring,
106 summer and autumn campaigns corresponded to the end of leaf growth, leaf maturation and the beginning of the
107 leaf senescence, respectively. The same five trees per plot were selected and investigated throughout the study.

2.2 Branch scale-sampling methods

Two identical dynamic branch enclosures were used for sampling gas exchange (in terms of CO_2, H_2O and BVOCs) as fully described in Genard-Zielinski *et al.* (2015) with some modifications. Branches were enclosed in a ≈ 30L PTFE (polytetrafluoroethylene) frame closed by a 50µm thick PTFE film. One tree from natural and one tree from amplified drought plot were analysed concomitantly during 1 or 2 days. Inlet air was introduced at 9L.min^{-1}, controlled by mass flow controllers (MFC, Bronkhorst), using a pump, inside, by PTFE (KNF N840.1.2FT.18®, Germany) allowing for air renewal inside the chamber every ~ 3min. Ozone was removed from inlet air by placing PTFE filters impregnated with sodium thiosulfate ($Na_2S_2O_3$) as described by Pollmann *et al.* (2005), so that oxidation of BVOCs due to ozone within the enclosed atmosphere is negligible. The excess of air humidity was removed using drierite. A PTFE fan ensured a rapid mixing of the chamber air and a slight positive pressure within the enclosure enabled the PTFE film to be held away from leaves to minimise biomass damage. Microclimate (temperature, relative humidity and photosynthetically active radiation or PAR) was continuously (every minute) monitored by a data logger (LI-COR 1400®; Lincoln, NE, USA) with a relative humidity and temperature probe placed inside the chamber (RHT probe, HMP60, Vaisala, Finland) and a quantum sensor (PAR, LI-COR, PAR-SA 190®, Lincoln, NE, USA) placed outside the chamber. The climatic conditions in terms of PAR and temperatures are summarized in Fig. S1 (in supplementary files) for each field campaigns. All air flow rates were controlled by mass flow controllers (MFC, Bronkhorst) and all tubing lines were made of PTFE. Chambers were installed the day before measurements and flushed overnight. Enclosed branches contained 8 to 12 leaves corresponding to a range of 1.4 to 3.6 g of dry matter and 110 to 320 cm² of leaf surface, respectively.

2.3 Ecophysiological parameters

Exchange of CO_2 and H_2O from the enclosed branches was continuously (every min) measured using infrared gas analysers (IRGA 840A®, LI-COR) concomitantly with BVOCs emission measurements (cf. 2.4). Gas exchange values were averaged by taking into account all the data measured between 12h and 15h (local time). Net photosynthesis (*Pn,* µmolCO_2 m^{-2} s^{-1}) and stomatal conductance to water (*Gw*, mmolH_2O m^{-2} s^{-1}) were calculated using equations described by Von Caemmerer and Farquhar (1981) as used in Genard-Zielinski *et al.* (2015) (for more details, see Appendix A, equations A1 to A4). Leaves from enclosed branches were directly collected after gas exchange sampling to accurately measure leaf surface with a leaf area meter. *Pn* and *Gw* were hence expressed in a leaf surface basis. After that, leaves were freeze-dried to assess their dry mass.

2.4 BVOCs analysis

A PTR-ToF-MS 8000 instrument (Ionicon Analytik GmbH, Innsbruck, Austria) was used for online measurements of BVOCs emitted by the enclosed branches. A multi-position common outlet flow path selector valve system (Vici) and a vacuum pump were used to sequentially select air samples from: amplified drought, inlet air, natural drought, ambient air and catalyst. The catalyst consists in a 25 cm long stainless steel tubing, filled with platinum wool and heated at 350°C to efficiently remove VOCs from sample and measure potential instrumental background levels. Each sample was analysed every hour, with 15min of analysis. Mass spectra in the range 0-500amu were recorded at 1min integration time. The reaction chamber pressure was fixed at 2.1mbar, the drift tube voltage at 550V and the drift tube temperature at 313 K corresponding to an electric field strength applied to the drift tube

145 (E) to a buffer gas density (N) ratio of 125Td (1Td = 10^{-17} V cm^2). A calibration gas standard, consisting of a
146 mixture of 14 aromatic organic compounds (TO-14A Aromatic Mix, Restek Corporation, Bellefonte, USA, 100 ±
147 10ppb in Nitrogen), was used to experimentally determine the ion relative transmission efficiency. BVOCs
148 targeted in this study and their corresponding ions include formaldehyde (m/z 31.018), methanol (m/z 33.033),
149 acetaldehyde (m/z 45.03), acetone (m/z 59.05), isoprene (m/z 41.038, 69.069) and MACR+MVK+ISOPOOH (m/z
150 71.049, these three compounds were detected with the same ion with PTR-MS). The signal corresponding to
151 protonated VOCs was converted into mixing ratios by using the proton transfer rate constants k given by Cappellin
152 *et al.* (2012). Formaldehyde concentrations were calculated according to the method described by Vlasenko *et al.*
153 (2010) to account for its humidity dependent sensitivity.
154 BVOCs emissions rates (ER) were calculated by considering the BVOCs concentrations in the inlet and outlet air
155 as follows (equation 1):

156 $$ER = \frac{Q_0 * (C_{out} - C_{in})}{B} \quad (1)$$

157 where *ER* was expressed in µgC g_{DM}^{-1} h^{-1}, Q_0 was the flow rate of the air introduced into the chamber (L h^{-1}), C_{out}
158 and C_{in} were the concentrations in the inflowing and outflowing air (µgC L^{-1}), respectively, and B was the total
159 dry biomass matter (g_{DM}). Daily cycles were made by averaging measured emissions of all trees every hour.

160 **2.5 Emission algorithms**

161 The light and/or temperature dependence of *Q. pubescens* BVOCs (isoprene and highly volatile compounds) under
162 natural and amplified drought was tested using both the *L+T* and *T* algorithms. Emission rates calculated according
163 to these algorithms (afterwards, called ER_{L+T} and ER_T, respectively) were calculated using the equations described
164 in Guenther *et al.* (1995) (for more details, see Appendix B, equations B1 to B5). The empirical coefficient β (used
165 in the *T* algorithm) was determined for each compound according to the season and the treatment through the slope
166 of correlation between the natural logarithm of emissions rates (measured emissions, µgC g_{DM}^{-1} h^{-1}) and
167 experimental temperature (K). Emissions factors (*EF*), that are emissions rates at standard conditions of light and
168 temperature, 1000µmol m^{-2} s^{-1} and 30°C), were used to calculate modelled emissions and were determined for each
169 compound under each season and treatment. *EF* values correspond to the slope of the correlation between
170 experimental emission rates and C_l*C_t when using the *L+T* algorithm or C_T when using the *T* algorithm (without
171 forcing data to pass through the origin, see Appendix B for a full description of C_l*C_t and C_T). All parameters used
172 for the calculation of modelled emissions are presented in supplementary files (Table S1 and S2).

173 **2.6 Data treatment**

174 Data treatment was performed with the software STATGRAPHICS® centurion XV (Statpoint, Inc). After having
175 checked the normality of the data set, two-way repeated measures ANOVA were carried out to evaluate the
176 variability of *Pn*, *Gw* and BVOC emission rates according to the drought treatment and season. Correlation
177 coefficient (R^2) and slope (called "sl" afterwards) from Pearson's correlations between measured and modelled
178 emissions were used to evaluate the algorithm (*L+T* or *T*) that better predicted *Q. pubescens* emissions under the
179 different drought conditions and seasonal cycle. The slope of those correlations indicate if there was an under- or
180 over- estimation of modelled emissions when sl < 1 and sl > 1, respectively. For that, slope comparison tests were

181 performed to check for slope significant differences from 1. These correlations were obtained without forcing data
182 to pass through the origin.

183 **3. Results and discussion**

184 **3.1 Ecophysiological parameters**

185 The physiology of *Q. pubescens* was slightly impacted by amplified drought over the whole study (Fig. 2), with a
186 decrease of *Gw* under amplified drought compared to natural drought – ranging from 44 % in spring ($P < 0.1$) to
187 55 % in summer ($P < 0.01$, Table 1). In autumn, there was no significant difference between both treatments. Pn
188 was only slightly reduced in summer by 36 % ($P < 0.1$) with no difference for the others season. Thus, the stomatal
189 closure observed had a slight impact on carbon assimilation. Indeed, *Q. pubescens* has a high stem hydraulic
190 efficiency (Nardini & Pitt 1999) which compensates stomatal closure since it allows to use water more efficiently,
191 thus, maintaining *Pn*. Moreover, it must be noted that an increase of *Pn* was observed in autumn and could likely
192 be attributed to autumnal rains. These results showed that the amplified drought artificially applied to *Q. pubescens*
193 at O_3HP led to a moderate drought for this species, based on a moderate reduction of the physiological
194 performances (Niinemets 2010).

195 **3.2 Effect of drought on BVOCs emissions**

196 Emissions of all BVOCs followed during this experimentation were reduced under amplified drought compared
197 to natural drought, especially in spring and summer (Table 1) except for acetaldehyde emissions. Indeed,
198 acetaldehyde was not significantly different between both treatments probably due to a large variability of the data
199 set. In autumn, for all BVOCs, there was no difference between both plots. The decrease of oxygenated BVOCs
200 in spring and summer under amplified drought (e.g. methanol, MACR+MVK+ISOPOOH, formaldehyde, acetone)
201 could be explained by stomatal closure in spring and summer under amplified drought since emissions of these
202 compounds are strongly bound to *Gw* (Niinemets *et al.* 2004). Isoprene emissions were also reduced in spring and
203 summer during the 3rd year of this experiment whereas an increase had been observed in the first year (Génard-
204 Zielinski *et al.* in prep) as well as what had been shown by Brüggemann and Schnitzler (2002) but this work was
205 conducted with potted plants. The isoprene decrease observed in our experiment cannot be explained by the
206 stomatal closure because this compound could also be emitted through the cuticle (Sharkey & Yeh 2001). It could
207 rather be due to the decrease of *Pn* which reduced the carbon availability to produce isoprene. Moreover, carbon
208 assimilated through *Pn* can be also invested into the synthesis of other defense compounds leading to a decrease
209 of isoprene production and emission.

210 **3.3 Effect of drought on light and/or temperature dependence through a seasonal cycle**

211 All six BVOCs monitored showed daytime light and temperature dependencies (isoprene, degradation products of
212 isoprene and acetaldehyde), while three BVOCs (methanol, acetone and formaldehyde) also showed emissions
213 during the night despite the absence of light under constant temperature.
214

215 Regarding the light and temperature dependencies, the daily cycle of isoprene emissions (Fig. 3) showed that this
216 compound clearly responds to light and temperature as already known (Guenther *et al.* 1993) and that this response
217 is not impacted by amplified drought. Isoprene can protect thylakoids from oxidative damage (Velikova *et al.*
218 2011) occurring mainly during the day which can explain this kind of dependence. Yet, our results show the
219 intensity of isoprene emission factor under natural and amplified drought is very different independently of the
220 season. The modelled emissions were very representative of measured emissions except in spring under natural
221 drought when we obtained a slight underestimation of emissions (sl = 0.84, $P < 0.05$) maybe, because light and
222 temperature, in spring, were not the only parameters driving isoprene emissions. At this season, plants likely
223 needed to produce more isoprene to protect the establishment of the photosynthetic machinery in the new leaves.
224 MACR+MVK+ISOPOOH emissions, as isoprene, seemed to respond better to light and temperature than to only
225 temperature (Fig. S2 in supplementary files) since correlations between measured emissions and ER_{L+T} were
226 always better than correlations with ER_T. Since MACR+MVK+ISOPOOH are oxidation products of isoprene
227 (Oikawa & Lerdau 2013), it is not surprising that these compounds followed the same pattern than isoprene in
228 terms of dependence to light and temperature. The estimations of ER_{L+T} were quite good except in spring under
229 natural drought where a slight underestimation was observed (sl = 0.87, $P < 0.05$).
230 The dependence of acetaldehyde emissions to light and/or temperature is very contrasted; studies have shown that
231 they are bound to both light and temperature (Jardine 2008; Fares *et al.* 2011) or to temperature only (Hayward *et*
232 *al.* 2004). Our results suggested that acetaldehyde emissions were mainly bound to light and temperature (Fig. 4).
233 Indeed, correlations between measured and ER_{L+T} were always better than with ER_T. However, some discrepancies
234 were observed. Under natural drought, underestimations were observed in spring and summer (sl = 0.72, and sl =
235 0.57, $P < 0.05$, respectively) whereas in autumn, there was a good estimation (sl = 0.86, $P > 0.05$). Under amplified
236 drought, underestimation was only observed in summer (sl = 0.80, $P < 0.05$). Daily cycles of acetaldehyde
237 emissions presented also an emissions burst in the morning (at 7h, local time) in spring (under both treatments)
238 and in summer (only under natural drought). Acetaldehyde can be produced due to an overflow of pyruvic acid
239 during light-dark transitions. Cytosolic pyruvic acid levels rise rapidly and it can be converted into acetaldehyde
240 by pyruvate decarboxylase (Fall 2003). This mechanism could explain the morning burst for this compound and
241 the fact that no emissions during the night was observed.
242
243 We observed emissions of methanol, acetone and formaldehyde during the night under no light and constant
244 temperature (around 20°C, see supplementary files S1). Correlations between ER_{L+T} or ER_T and measured
245 methanol emissions were very similar especially in spring and summer (Fig. 5). However, some observed
246 phenomena suggested that methanol emission was sustained by temperature in the absence of light. Indeed, the
247 burst in the early morning (at 7h, local time), similar to acetaldehyde, was observed when stomata opened in spring
248 and summer, independently of the drought treatment although it was clearer under natural than amplified drought.
249 This burst can be explained by a strong release of this compound that has been accumulated in the intercellular air
250 space and leaf liquid pools (due to the relative high polarity of methanol) at night when stomata are closed (Hüve
251 *et al.* 2007). Moreover, for both drought treatments, methanol emissions during the night were observed at any
252 seasons (especially autumn) which could be explained by nocturnal temperatures (roughly constant) that sufficed
253 to maintain the biochemical processes involved in methanol formation. Methanol emissions, which result from the
254 demethylation of pectin during the leaf elongation, has already been described to be temperature dependent alone

255 (Hayward *et al.* 2004; Folkers *et al.* 2008). However, our results suggest that methanol emissions respond strongly
256 to light and temperature during the day. This kind of diurnal emissions cycle has already been described by Smiatek
257 and Steinbrecher (2006). Our results about daily cycles of acetone emissions (Fig. S3 in supplementary files)
258 showed that this compound responded better to light and temperature than only temperature since correlations
259 were better with ER_{L+T}. Under natural drought, the modelled emissions were well representative of measured
260 emissions in summer. By contrast, in spring and in autumn, slight underestimations were observed (sl = 0.88, $P <$
261 0.05 and sl = 0.69, $P < 0.05$, respectively). Under amplified drought, good estimations were observed in summer
262 and autumn but in spring, there was an overestimation of modelled emissions (sl = 1.27, $P < 0.05$). Previous studies
263 have shown that acetone rather depends on temperature alone (Fares *et al.* 2011) or to light and temperature (Jacob
264 *et al.* 2002), indicating that its dependence on light and/or temperature remains unclear. During the day, acetone
265 emissions were dependent on light and temperature and emissions still occurred during the night, especially in
266 autumn. Alike methanol, nocturnal temperatures could allow to maintain acetone formation (Smiatek &
267 Steinbrecher 2006). Acetone is a by-product of plant metabolism (Jacob *et al.* 2002) and its production can be
268 enzymatic and non-enzymatic (Fall 2003) which can explain these observed differences through the day. We can
269 suppose that acetone emissions observed during the day could come from the enzymatic activity and, on the
270 contrary, during the night, they could come from the non-enzymatic production.
271 Formaldehyde emissions followed the same pattern than methanol and acetone emissions (Fig. S4 in
272 supplementary files), especially in autumn. By considering only the daytime (correlation with $L+T$ modelled
273 emissions), there were good estimations in summer and autumn and a slight underestimation was observed in
274 spring (sl = 0.89, $P < 0.05$) for natural drought. Under amplified drought, correlations indicated that $L+T$ modelled
275 emissions were well representative of measured emissions, but some negative emissions were observed in summer
276 which suggested a deposition or an uptake of this compound by leaves as already highlighted by Seco *et al.* (2008).
277 This phenomenon could have a role in stress tolerance, since formaldehyde can be catabolised (mainly through
278 oxidations) within leaves leading to CO_2 formation (Oikawa & Lerdau 2013). Emissions during the night suggest
279 that formaldehyde came from another source than oxidation within leaves since oxidations occur mainly during
280 the day due to an excess of light in chloroplasts, principal place of reactive oxygen species production (Asada
281 2006). Thus, formaldehyde emissions observed during the night could result from, for example, the glyoxylate
282 decarboxylation or the dissociation of 5,10-methylene-THF (Oikawa & Lerdau 2013).
283 Predicting emissions rates of these 3 compounds (methanol, acetone and formaldehyde), during the night, seem to
284 require other parameters such as a temperature threshold, below which methanol, acetone and formaldehyde
285 synthesis and so emissions do not occur (Ghirardo *et al.* 2010).

286 **4 Conclusion**

287 After 3 years of amplified drought, all BVOC emissions were reduced in spring and summer compared to natural
288 drought whereas, in autumn, an increase was observed for some compounds. These results are in opposition with
289 the results obtained after only one year of amplified drought (2012), especially for isoprene, where an increase
290 was observed for this compound (Génard-Zielinski *et al.* in prep). Amplified drought did not seem to shift the
291 dependence to light and/or temperature which remained unchanged between treatments.

292 Moreover, two different dependence behaviours were found: (i) all six BVOCs monitored showed daytime light
293 and temperature dependencies while (ii) only three BVOCs (methanol, acetone and formaldehyde) also showed
294 that their emissions were maintained during the night with no light at rather constant nocturnal temperatures.
295 Moreover, some phenomena, such as methanol and acetaldehyde emissions bursts in early morning or the
296 formaldehyde deposition/uptake (formaldehyde), were not assessed by either *L+T* or *T* algorithm.

297 Appendix A: calculation of ecophysiological parameters

298 Net photosynthesis (*Pn*, µmolCO_2 m^{-2} s^{-1}) was calculated using equations described by Von Caemmerer and
299 Farquhar (1981) as follows:

300 $$\mathrm{Pn} = \frac{F*(Cr-Cs)}{S} - CS*E \quad \text{(A1)}$$

301 Where *F* is the inlet air flow (mol s^{-1}), *Cs* and *Cr* are the sample and reference CO_2 molar fraction respectively
302 (ppm), *S* is the leaf surface (m²), *Cs*E* is the fraction of CO_2 diluted in water evapotranspiration and *E* (molH_2O
303 m^{-2} s^{-1} then transformed in mmolH_2O m^{-2} s^{-1}, afterward) is the transpiration rate calculated as follow:

304 $$\mathrm{E} = \frac{F*(Ws-Wr)}{S*(1-Ws)} \quad \text{(A2)}$$

305 where *Ws* and *Wr* are the sample and the reference H_2O molar fraction respectively (molH_2O mol^{-1}).
306 Stomatal conductance to water (*Gw*, molH_2O m^{-2} s^{-1} then transformed in mmolH_2O m^{-2} s^{-1}) was calculated using
307 the following equation:

308 $$\mathrm{Gw} = \frac{E*(1-\frac{Wl-Ws}{2})}{Wl-Ws} \quad \text{(A3)}$$

309 where *Wl* is the molar concentration of water vapour within the leaf (molH_2O mol^{-1}) calculated as follows:

310 $$Wl = \frac{Vpsat}{P} \quad \text{(A4)}$$

311 where Vpsat is the saturated vapour pressure (kPa) and P was the atmospheric pressure (kPa).

312 Appendix B: Modelled emissions calculation

313 The modelled emissions rates according to light and temperature (ER_{L+T}) or the temperature algorithm (ER_T) were
314 calculated according to algorithms described in Guenther *et al.* (1995) as follows :

315 $$ER_{L+T} = EF_{L+T} * Cl * Ct \quad \text{(B1)}$$

316 where EF_{L+T} is the emission factor at 1000 µmol m^{-2} s^{-1} of photosynthetically active radiation (PAR) and 30°C of
317 temperature (obtained with the slope of the correlation between experimental emissions and *Cl* **Ct* without forcing
318 data to pass through the origin), *Cl* and *Ct* correspond to light and temperature dependence factors respectively
319 and were calculated with the following formulae:

320 $$Cl = \frac{\alpha C_{L1} L}{\sqrt{1+\alpha^2 L}} \quad \text{(B2)}$$

321 $$Ct = \frac{exp\,\frac{C_{T1}(T-T_S)}{RT_S T}}{1+exp\frac{C_{T2}(T-T_M)}{RT_S T}} \quad \text{(B3)}$$

322 where α = 0.0027, C_{L1} = 1.066, C_{T1} = 95000J mol^{-1}, C_{T2} =230000J mol^{-1}, T_M = 314K are empirically derived
323 constants, L is the photosynthetically active radiation (PAR) flux (µmol m^{-2} s^{-1}), T is the leaf experimental
324 temperature (K) and T_S is the leaf temperature at standard condition (303K).
325 Modelled emissions according to temperature alone that is ER_T, was calculated as follows:

326 $$ER_T = EF_T * C_T \quad \text{(B4)}$$

327 where EF_T is the emission factor at 30°C of temperature (obtained with the slope of the correlation between
328 experimental emissions and C_T without forcing data to pass through the origin) and C_T is a temperature dependence
329 factor calculated as follows:

330 $$C_T = \exp[\beta(T - T_S)] \quad \text{(B5)}$$

331 where β is an empirical coefficient (with a standard variation value of 0.09K^{-1} used in literature when not measured)
332 determined, in this study, for each compound according to the season and the treatment through the slope of the
333 correlation between the natural logarithm of measured emissions rates (ER, µgC g_{DM}^{-1} h^{-1}) and experimental
334 temperature (expressed in K), T is the leaf experimental temperature (K) and T_S is the standard temperature (303K).

335 **Author contribution**

336 AS, EO and CF designed the research and the experimental design. AS, BTR, EO and CF conducted the research.
337 AS, CB, BTR, and CL collected and analyzed the data. AS, EO, CB, HW, BTR, AA and CF wrote the manuscript

338 **Competing interests**

339 The authors declare that they have no conflict of interest.

340 **Acknowledgments**

341 This work was supported by the French National Agency for Research (ANR) through the SecPriMe² project
342 (ANR-12-BSV7-0016-01); Europe (FEDER) and ADEME/PACA for PhD funding. We are grateful to FR3098
343 ECCOREV for the O_3HP facilities (https://o3hp.obs-hp.fr/index.php/fr/). We are very grateful to J.-P. Orts, I.
344 Reiter. We also thank all members of the DFME team from IMBE and particularly: S. Greff, S. Dupouyet and A.
345 Bousquet-Melou for their help during measurements and analysis. We thank also, the Université Paris Diderot-
346 Paris7 for its support. The authors thank the MASSALYA instrumental platform (Aix Marseille Université,
347 lce.univ-amu.fr) for the analysis and measurements used in this publication.

348 **References**

349 Arneth A., Monson R., Schurgers G., Niinemets Ü. & Palmer P. (2008). Why are estimates of global terrestrial
350 isoprene emissions so similar (and why is this not so for monoterpenes)? *Atmospheric Chemistry and*
351 *Physics*, 8, 4605-4620.
352 Asada K. (2006). Production and scavenging of reactive oxygen species in chloroplasts and their functions. *Plant*
353 *physiology*, 141, 391-396.
354 Beauchamp J., Wisthaler A., Hansel A., Kleist E., Miebach M., NIINEMETS Ü., Schurr U. & WILDT J. (2005).
355 Ozone induced emissions of biogenic VOC from tobacco: relationships between ozone uptake and
356 emission of LOX products. *Plant, Cell & Environment*, 28, 1334-1343.

Brüggemann N. & Schnitzler J.P. (2002). Comparison of Isoprene Emission, Intercellular Isoprene Concentration and Photosynthetic Performance in Water-Limited Oak (Quercus pubescens Willd. and Quercus robur L.) Saplings. *Plant Biology*, 4, 456-463.

Cappellin L., Karl T., Probst M., Ismailova O., Winkler P.M., Soukoulis C., Aprea E., Märk T.D., Gasperi F. & Biasioli F. (2012). On quantitative determination of volatile organic compound concentrations using proton transfer reaction time-of-flight mass spectrometry. *Environmental science & technology*, 46, 2283-2290.

Dindorf T., Kuhn U., Ganzeveld L., Schebeske G., Ciccioli P., Holzke C., Köble R., Seufert G. & Kesselmeier J. (2006). Significant light and temperature dependent monoterpene emissions from European beech (Fagus sylvatica L.) and their potential impact on the European volatile organic compound budget. *Journal of Geophysical Research: Atmospheres*, 111.

Fall R. (2003). Abundant oxygenates in the atmosphere: a biochemical perspective. *Chemical reviews*, 103, 4941-4952.

Fares S., Gentner D.R., Park J.-H., Ormeno E., Karlik J. & Goldstein A.H. (2011). Biogenic emissions from< i> Citrus</i> species in California. *Atmospheric Environment*, 45, 4557-4568.

Folkers A., Hüve K., Ammann C., Dindorf T., Kesselmeier J., Kleist E., Kuhn U., Uerlings R. & Wildt J. (2008). Methanol emissions from deciduous tree species: dependence on temperature and light intensity. *Plant biology*, 10, 65-75.

Fortunati A., Barta C., Brilli F., Centritto M., Zimmer I., Schnitzler J.P. & Loreto F. (2008). Isoprene emission is not temperature‐dependent during and after severe drought‐stress: a physiological and biochemical analysis. *The Plant Journal*, 55, 687-697.

Funk J., Mak J. & Lerdau M. (2004). Stress‐induced changes in carbon sources for isoprene production in Populus deltoides. *Plant, Cell & Environment*, 27, 747-755.

Genard-Zielinski A.-C., Boissard C., Fernandez C., Kalogridis C., Lathière J., Gros V., Bonnaire N. & Ormeño E. (2015). Variability of BVOC emissions from a Mediterranean mixed forest in southern France with a focus on Quercus pubescens. *Atmospheric Chemistry and Physics Discussions*, 14, 17225-17261.

Ghirardo A., Koch K., Taipale R., Zimmer I., SCHNITZLER J.P. & Rinne J. (2010). Determination of de novo and pool emissions of terpenes from four common boreal/alpine trees by 13CO2 labelling and PTR‐MS analysis. *Plant, cell & environment*, 33, 781-792.

Giorgi F. & Lionello P. (2008). Climate change projections for the Mediterranean region. *Global and Planetary Change*, 63, 90-104.

Guenther A., Hewitt C.N., Erickson D., Fall R., Geron C., Graedel T., Harley P., Klinger L., Lerdau M., McKay W.A., Pierce T., Scholes B., Steinbrecher R., Tallamraju R., Taylor J. & Zimmerman P. (1995). A global model of natural volatile organic compound emissions. *Journal of Geophysical Research: Atmospheres*, 100, 8873-8892.

Guenther A., Jiang X., Heald C., Sakulyanontvittaya T., Duhl T., Emmons L. & Wang X. (2012). The Model of Emissions of Gases and Aerosols from Nature version 2.1 (MEGAN2. 1): an extended and updated framework for modeling biogenic emissions.

Guenther A., Karl T., Harley P., Wiedinmyer C., Palmer P. & Geron C. (2006). Estimates of global terrestrial isoprene emissions using MEGAN (Model of Emissions of Gases and Aerosols from Nature). *Atmospheric Chemistry and Physics*, 6, 3181-3210.

Guenther A.B., Zimmerman P.R., Harley P.C., Monson R.K. & Fall R. (1993). Isoprene and monoterpene emission rate variability: model evaluations and sensitivity analyses. *Journal of Geophysical Research: Atmospheres (1984–2012)*, 98, 12609-12617.

Hallquist M., Wenger J., Baltensperger U., Rudich Y., Simpson D., Claeys M., Dommen J., Donahue N., George C. & Goldstein A. (2009). The formation, properties and impact of secondary organic aerosol: current and emerging issues. *Atmospheric Chemistry and Physics*, 9, 5155-5236.

Harrison S.P., Morfopoulos C., Dani K., Prentice I.C., Arneth A., Atwell B.J., Barkley M.P., Leishman M.R., Loreto F. & Medlyn B.E. (2013). Volatile isoprenoid emissions from plastid to planet. *New Phytol.*, 197, 49-57.

Hayward S., Tani A., Owen S.M. & Hewitt C.N. (2004). Online analysis of volatile organic compound emissions from Sitka spruce (Picea sitchensis). *Tree Physiology*, 24, 721-728.

Heikes B.G., Chang W., Pilson M.E., Swift E., Singh H.B., Guenther A., Jacob D.J., Field B.D., Fall R. & Riemer D. (2002). Atmospheric methanol budget and ocean implication. *Global Biogeochemical Cycles*, 16, 80-1-80-13.

Hüve K., Christ M., Kleist E., Uerlings R., Niinemets Ü., Walter A. & Wildt J. (2007). Simultaneous growth and emission measurements demonstrate an interactive control of methanol release by leaf expansion and stomata. *Journal of experimental botany*, 58, 1783-1793.

IPCC (2013). In: *Contribution of working group I to the fith assessment report of the intergovernmental panel on climate change*. Cambridge Univeristy Press Cambridge.

417 Jacob D.J., Field B.D., Jin E.M., Bey I., Li Q., Logan J.A., Yantosca R.M. & Singh H.B. (2002). Atmospheric
418 budget of acetone. *Journal of Geophysical Research: Atmospheres (1984–2012)*, 107, ACH 5-1-ACH
419 5-17.
420 Jardine J. (2008). Plant physiological and environmental controls over the exchange of acetaldehyde between
421 forest canopies and the atmosphere. *Biogeosciences*, 5.
422 Jimenez J., Canagaratna M., Donahue N., Prevot A., Zhang Q., Kroll J.H., DeCarlo P.F., Allan J.D., Coe H. &
423 Ng N. (2009). Evolution of organic aerosols in the atmosphere. *Science*, 326, 1525-1529.
424 Keenan T., Niinemets Ü., Sabate S., Gracia C. & Peñuelas J. (2009). Process based inventory of isoprenoid
425 emissions from European forests: model comparisons, current knowledge and uncertainties.
426 *Atmospheric Chemistry and Physics Discussions*, 9, 6147-6206.
427 Kesselmeier J. & Staudt M. (1999). Biogenic volatile organic compounds (VOC): an overview on emission,
428 physiology and ecology. *Journal of Atmospheric Chemistry*, 33, 23-88.
429 Lippmann M. (1989). Health effects of ozone a critical review. *Japca*, 39, 672-695.
430 Liu Y., Siekmann F., Renard P., El Zein A., Salque G., El Haddad I., Temime-Roussel B., Voisin D., Thissen R.
431 & Monod A. (2012). Oligomer and SOA formation through aqueous phase photooxidation of
432 methacrolein and methyl vinyl ketone. *Atmospheric Environment*, 49, 123-129.
433 Menut L., Bessagnet B., Khvorostyanov D., Beekmann M., Blond N., Colette A., Coll I., Curci G., Foret G. &
434 Hodzic A. (2014). CHIMERE 2013: a model for regional atmospheric composition modelling.
435 *Geoscientific Model Development*, 6, 981-1028.
436 Millet D.B., Guenther A., Siegel D.A., Nelson N.B., Singh H.B., de Gouw J.A., Warneke C., Williams J.,
437 Eerdekens G. & Sinha V. (2010). Global atmospheric budget of acetaldehyde: 3-D model analysis and
438 constraints from in-situ and satellite observations. *Atmospheric Chemistry and Physics*, 10, 3405-3425.
439 Monson R.K., Trahan N., Rosenstiel T.N., Veres P., Moore D., Wilkinson M., Norby R.J., Volder A., Tjoelker
440 M.G. & Briske D.D. (2007). Isoprene emission from terrestrial ecosystems in response to global
441 change: minding the gap between models and observations. *Philosophical Transactions of the Royal*
442 *Society of London A: Mathematical, Physical and Engineering Sciences*, 365, 1677-1695.
443 Nardini A. & Pitt F. (1999). Drought resistance of Quercus pubescens as a function of root hydraulic
444 conductance, xylem embolism and hydraulic architecture. *New Phytol.*, 143, 485-493.
445 Niinemets Ü. (2010). Mild versus severe stress and BVOCs: thresholds, priming and consequences. *Trends in*
446 *plant science*, 15, 145-153.
447 Niinemets Ü., Loreto F. & Reichstein M. (2004). Physiological and physicochemical controls on foliar volatile
448 organic compound emissions. *Trends in plant science*, 9, 180-186.
449 Oikawa P.Y. & Lerdau M.T. (2013). Catabolism of volatile organic compounds influences plant survival. *Trends*
450 *in plant science*, 18, 695-703.
451 Ormeno E., Goldstein A. & Niinemets Ü. (2011). Extracting and trapping biogenic volatile organic compounds
452 stored in plant species. *TrAC Trends in Analytical Chemistry*, 30, 978-989.
453 Owen S., Harley P., Guenther A. & Hewitt C. (2002). Light dependency of VOC emissions from selected
454 Mediterranean plant species. *Atmospheric environment*, 36, 3147-3159.
455 Papiez M.R., Potosnak M.J., Goliff W.S., Guenther A.B., Matsunaga S.N. & Stockwell W.R. (2009). The
456 impacts of reactive terpene emissions from plants on air quality in Las Vegas, Nevada. *Atmospheric*
457 *Environment*, 43, 4109-4123.
458 Polade S.D., Pierce D.W., Cayan D.R., Gershunov A. & Dettinger M.D. (2014). The key role of dry days in
459 changing regional climate and precipitation regimes. *Scientific reports*, 4.
460 Pollmann J., Ortega J. & Helmig D. (2005). Analysis of atmospheric sesquiterpenes: Sampling losses and
461 mitigation of ozone interferences. *Environmental science & technology*, 39, 9620-9629.
462 Quézel P. & Médail F. (2003). *Ecologie et biogéographie des forêts du bassin méditerranéen*. Elsevier Paris.
463 Reig-Armiñana J., Calatayud V., Cerveró J., Garcıa-Breijo F., Ibars A. & Sanz M. (2004). Effects of ozone on
464 the foliar histology of the mastic plant (Pistacia lentiscus L.). *Environmental Pollution*, 132, 321-331.
465 Rinne H., Guenther A., Greenberg J. & Harley P. (2002). Isoprene and monoterpene fluxes measured above
466 Amazonian rainforest and their dependence on light and temperature. *Atmospheric Environment*, 36,
467 2421-2426.
468 Seco R., Penuelas J. & Filella I. (2008). Formaldehyde emission and uptake by Mediterranean trees *Quercus ilex*
469 and *Pinus halepensis*. *Atmospheric Environment*, 42, 7907-7914.
470 Sharkey T.D. & Yeh S. (2001). Isoprene emission from plants. *Annual review of plant biology*, 52, 407-436.
471 Singh H., Chen Y., Tabazadeh A., Fukui Y., Bey I., Yantosca R., Jacob D., Arnold F., Wohlfrom K. & Atlas E.
472 (2000). Distribution and fate of selected oxygenated organic species in the troposphere and lower
473 stratosphere over the Atlantic. *Journal of Geophysical Research: Atmospheres (1984–2012)*, 105, 3795-
474 3805.
475 Smiatek G. & Steinbrecher R. (2006). Temporal and spatial variation of forest VOC emissions in Germany in the
476 decade 1994–2003. *Atmospheric Environment*, 40, 166-177.

477 Velikova V., Várkonyi Z., Szabó M., Maslenkova L., Nogues I., Kovács L., Peeva V., Busheva M., Garab G. &
478 Sharkey T.D. (2011). Increased thermostability of thylakoid membranes in isoprene-emitting leaves
479 probed with three biophysical techniques. *Plant Physiology*, 157, 905-916.
480 Vlasenko A., Macdonald A., Sjostedt S. & Abbatt J. (2010). Formaldehyde measurements by Proton transfer
481 reaction–Mass Spectrometry (PTR-MS): correction for humidity effects. *Atmospheric Measurement*
482 *Techniques*, 3, 1055-1062.
483 Von Caemmerer S.v. & Farquhar G. (1981). Some relationships between the biochemistry of photosynthesis and
484 the gas exchange of leaves. *Planta*, 153, 376-387.
485 Xie X., Shao M., Liu Y., Lu S., Chang C.-C. & Chen Z.-M. (2008). Estimate of initial isoprene contribution to
486 ozone formation potential in Beijing, China. *Atmospheric Environment*, 42, 6000-6010.

487

488

489

490

491

492

493

494

495

496

497

498

499

500

501

502

503

504

505

506

507

508

509

510 **Table:**

511 **Table 1: N**et photosynthesis (*Pn*, µmolCO_2 m^{-2} s^{-1}), stomatal conductance to water (*Gw*, mmolH_2O m^{-2} s^{-1}) and emission rates (µgC g_{DM}^{-1} h^{-1}) according to treatment and season.
512 Values represent an average of all data measured between 12h and 15h (local time). Letters denote the difference between drought treatments with a > b and values showed
513 represent the mean ± SE, n=5. ND: natural drought and AD: amplified drought with ns = non-significant, (*) = 0.05 < P < 0.1, * = 0.01 < P < 0.05, ** = 0.001 < P < 0.01,

Season	**Spring**			**Summer**			**Autumn**		
Treatments	**ND**	**AD**	***P***	**ND**	**AD**	***P***	**ND**	**AD**	***P***
Pn	11 ± 1 a	9 ± 2 a	ns	14 ± 2 a	9±1.2 b	(*)	7 ± 1 a	9 ± 1 a	ns
Gw	110 ± 19 a	57 ± 13 b	(*)	285 ± 38 a	126 ± 17 b	**	122 ± 23 a	74 ± 21 a	ns
Isoprene	20 ± 4 a	10 ± 2 b	*	124 ± 10 a	81 ± 11 b	*	3 ± 1 a	5 ± 2 a	ns
MACR+MVK+ISOPOOH	0.1 ± 0.03a	0.1 ± 0.01 a	ns	0.4 ± 0.1 a	0.2 ± 0.02 b	*	0.04 ± 0.01 a	0.1 ± 0.01 a	ns
Methanol	1 ± 0.1 a	0.5 ±0.04 b	*	1 ± 0.2 a	0.6 ± 0.03 b	*	0.2 ± 0.03 a	0.2 ± 0.1 a	ns
Acetaldehyde	1 ± 0.4 a	1 ± 0.3 a	ns	2 ± 0.5 a	1 ± 0.1 a	ns	1 ± 0.3 a	1 ± 0.3 a	ns
Acetone	0.5 ± 0.1 a	0.2 ± 0.02 a	ns	1 ± 0.2 a	0.5 ± 0.04 b	**	0.4 ± 0.1 a	0.4 ± 0.1 a	ns
Formaldehyde	0.2 ± 0.05 a	0.1 ± 0.01 a	ns	0.4 ± 0.1 a	0.1 ± 0.02 b	**	0.2 ± 0.1 a	0.3 ± 0.1 a	ns

514

515 **Figure legends**

516 **Figure 1**: Ombrothermic diagram for natural and amplified drought in 2012, 2013 and 2014. Bars represent mean
517 monthly precipitation (mm) and curves represent mean monthly temperature (°C). On each amplified drought
518 graph, the percentage represents the proportion of excluded rain compared to the natural drought plot.
519

520 **Figure 2**: Diurnal pattern of stomatal conductance (*Gw*) and net photosynthesis (*Pn*) according to drought
521 treatment and season**.** Values showed represent means ± SE, n=5.
522

523 **Figure 3**: Diurnal pattern of isoprene emissions rates, where points represent measured emission and the yellow
524 line corresponds to modelled emissions rates according to the *L*+*T* algorithm (ER_{L+T}). R^2 and slope (sl) of
525 correlations between measured and modelled emissions are presented in the yellow frame. Correlations were
526 obtained without forcing data to pass through the origin. Values are mean ± SE, n=5.
527

528 **Figure 4**: Diurnal pattern of acetaldehyde emissions rates, where points represent measured emission, the yellow
529 line corresponds to modelled emissions rates according to the *L*+*T* algorithm (ER_{L+T}) and the dotted line
530 corresponds to modelled emissions rates according to the *T* algorithm (ER_T). R^2 and slope (sl) of correlations
531 between measured and modelled emissions are presented in the yellow frame for *L*+*T* and in the white frame for
532 *T*. Correlations were obtained without forcing data to pass through the origin. Values are mean ± SE, n=5.
533

534 **Figure 5**: Diurnal pattern of measured methanol emissions rates. Points represent measured emission, the yellow
535 line corresponds to modelled emissions rates according to the *L*+*T* algorithm (ER_{L+T}) and the dotted line
536 corresponds to modelled emissions rates according to the *T* algorithm (ER_T). R^2 and slope (sl) of correlations
537 between measured and modelled emissions are presented in the yellow frame for *L*+*T* and in the white frame for
538 *T*. Correlations were obtained without forcing data to pass through the origin. Values are mean ± SE, n=5.
539
540
541
542
543
544
545
546
547
548
549
550

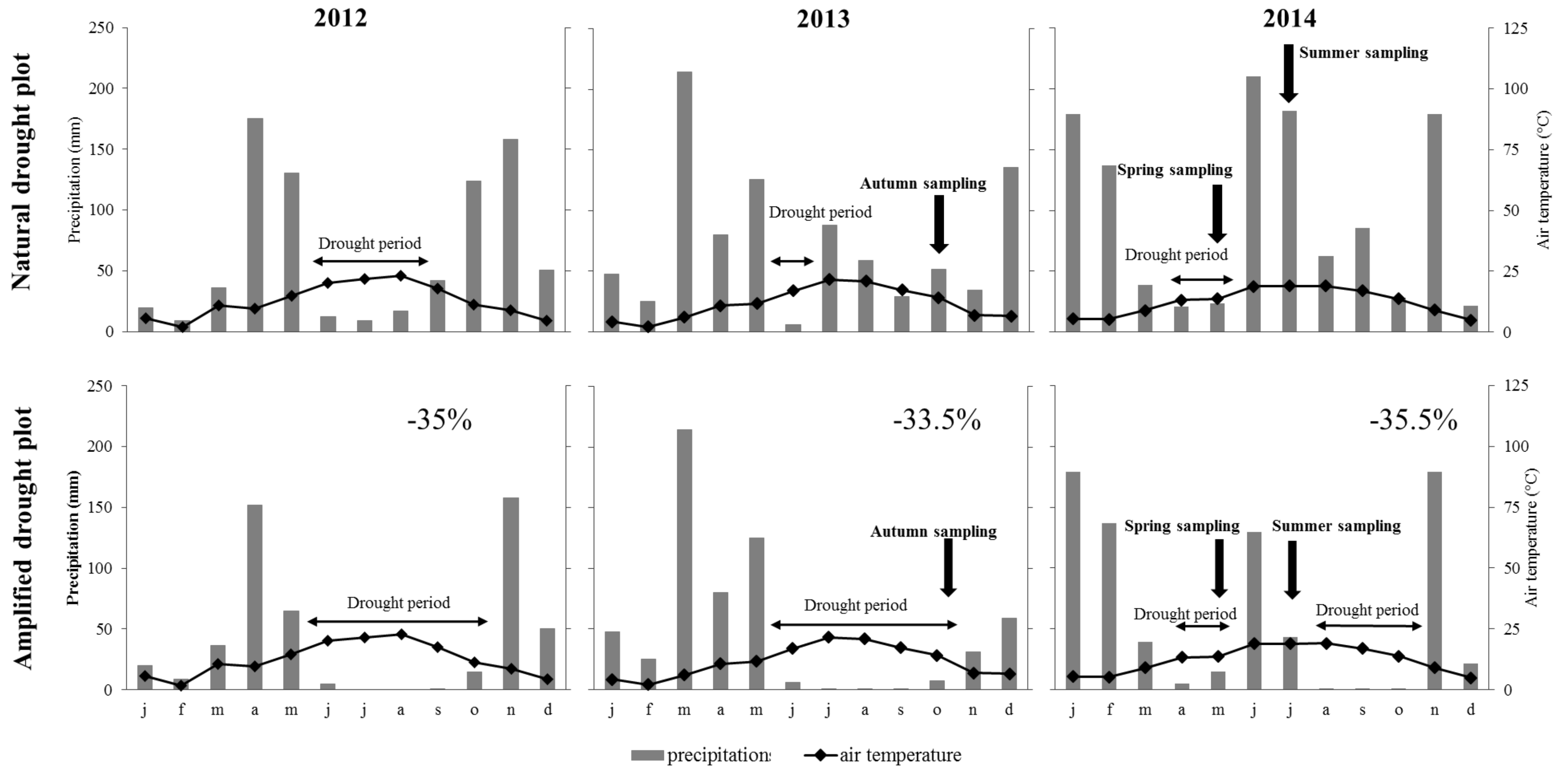

551

552 **Figure 1:**

553

554

555

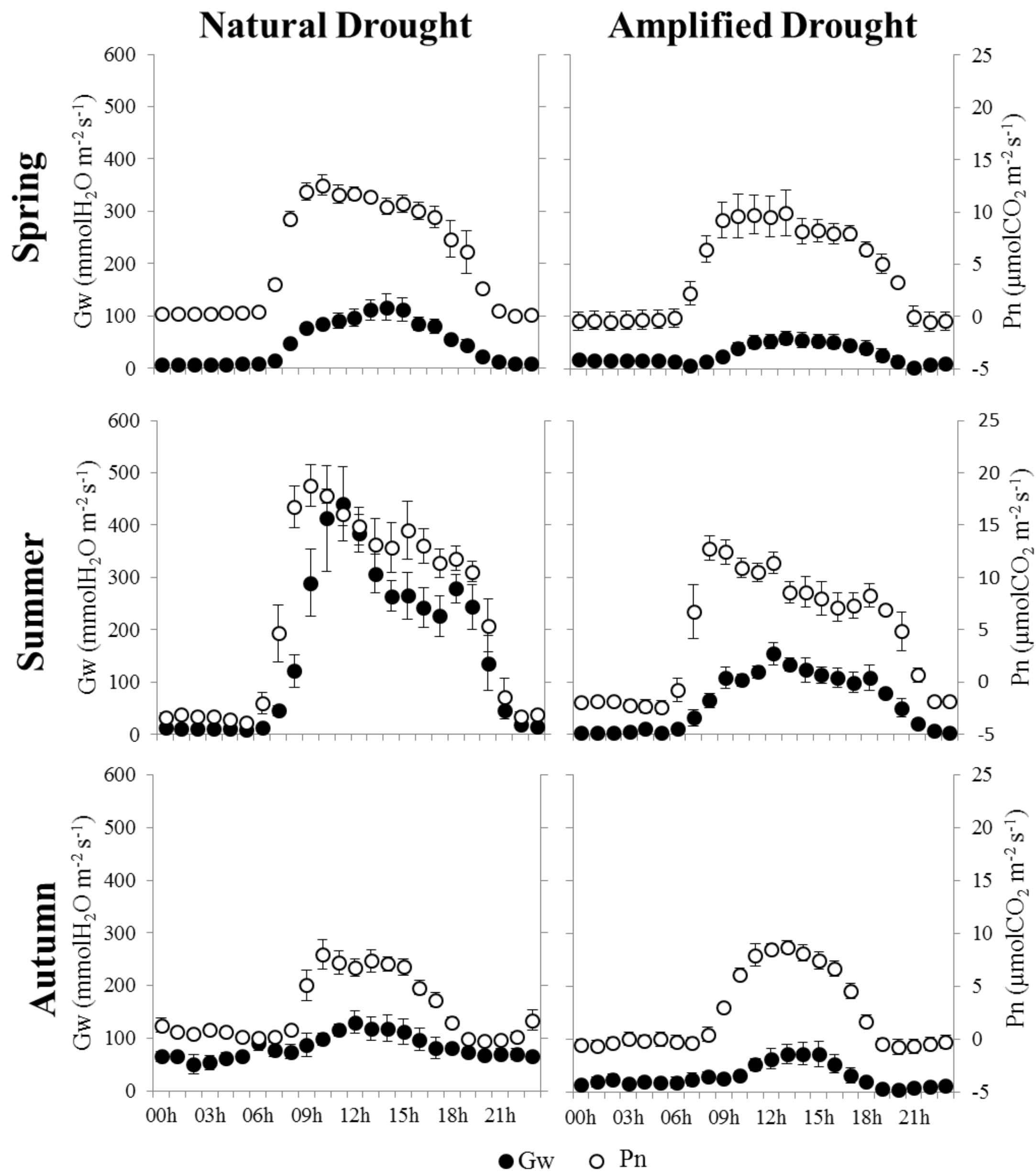

556

557 **Figure 2:**

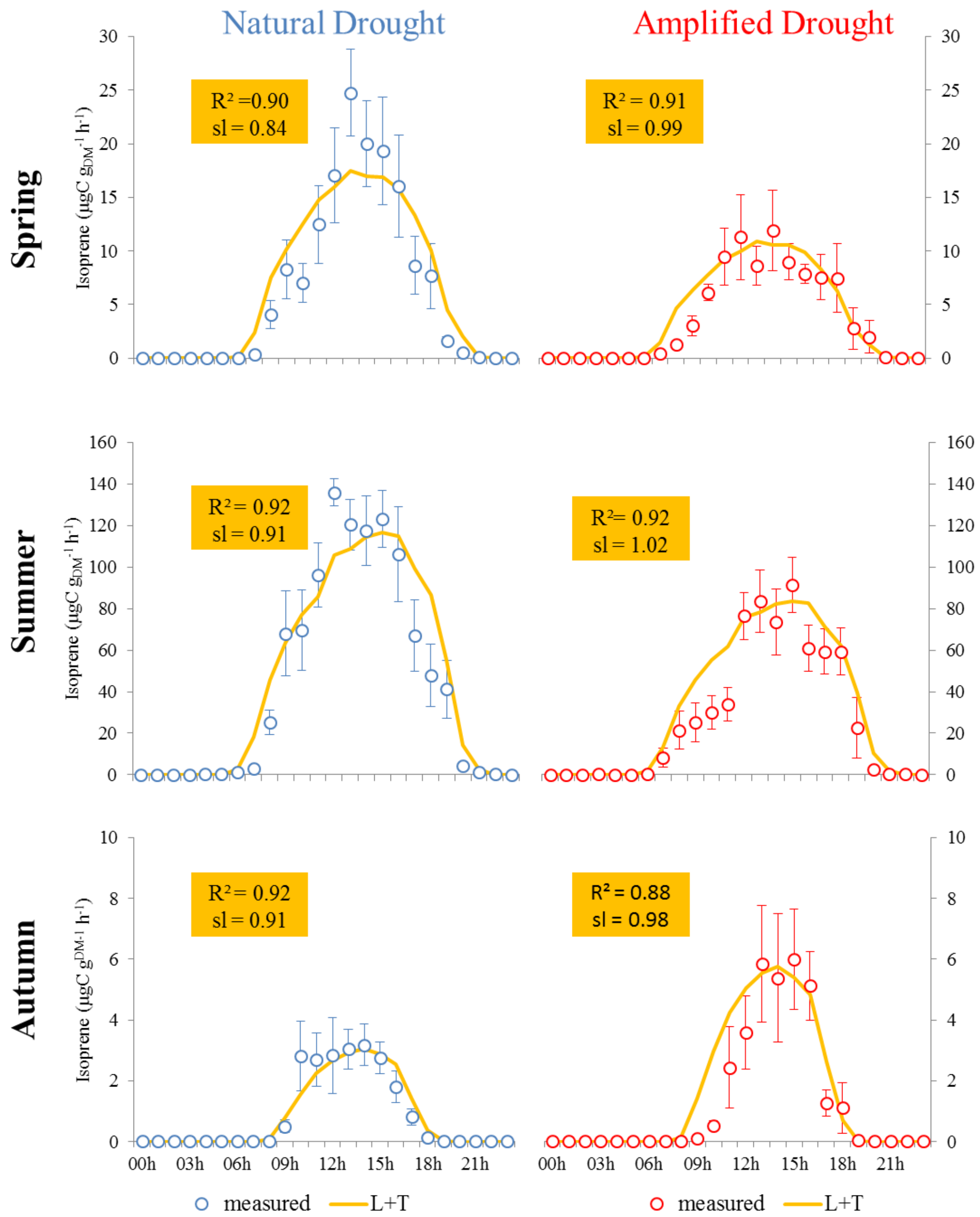

558

559 **Figure 3:**

560

561

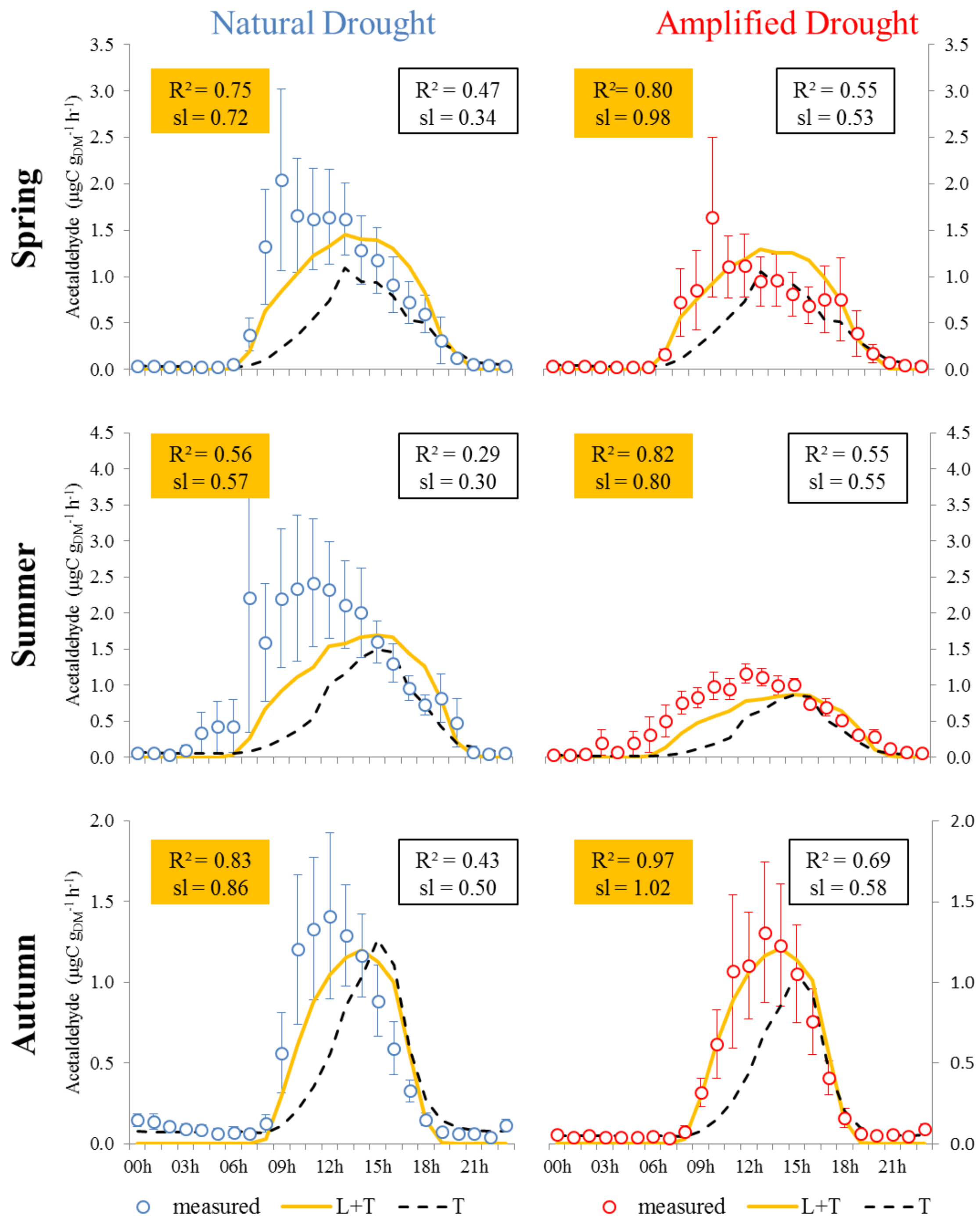

562

563 **Figure 4:**

564

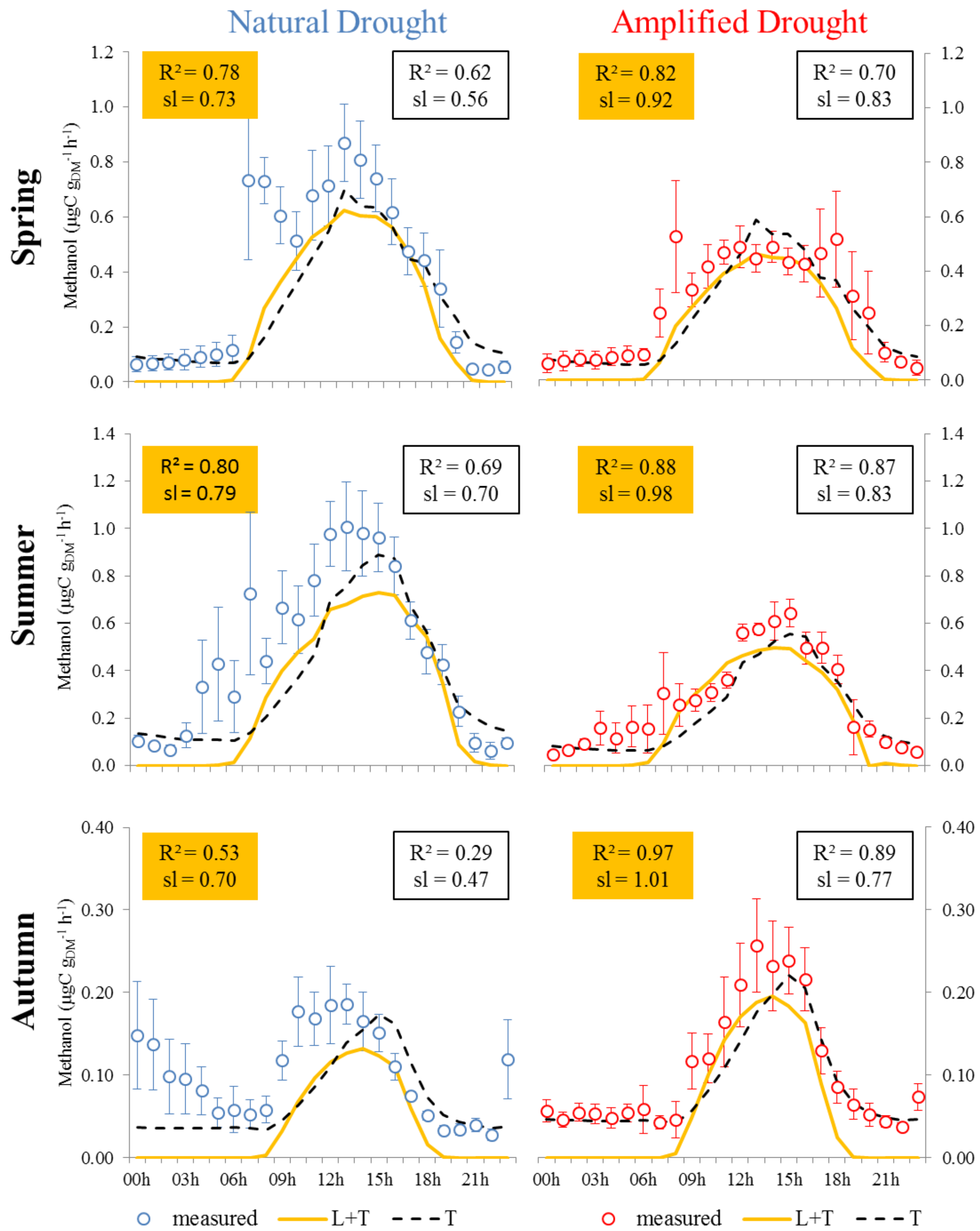

565

566 **Figure 5:**

567

568

569

570

571